

Article

A MODIS-Based Retrieval Model of Suspended Particulate Matter Concentration for the Two Largest Freshwater Lakes in China

Fangyuan Chen ¹, Guofeng Wu ^{1,2,3,*}, Junjie Wang ^{2,3}, Junjun He ^{1,4} and Yihan Wang ^{1,5}

¹ School of Resource and Environmental Sciences & Key Laboratory of Geographic Information System of the Ministry of Education, Wuhan University, Wuhan 430079, China; fangyuanchen@whu.edu.cn (F.C.); junjun.he@whu.edu.cn (J.H.); wangiyan@whu.edu.cn (Y.W.)

² Key Laboratory for Geo-Environmental Monitoring of Coastal Zone of the National Administration of Surveying, Mapping and GeoInformation & Shenzhen Key Laboratory of Spatial Smart Sensing and Services, Shenzhen University, Shenzhen 518060, China; wang_2015@szu.edu.cn

³ College of Life Sciences and Oceanography, Shenzhen University, Shenzhen 518060, China

⁴ Fourth Surveying and Mapping Institute of Anhui Province, Hefei 230031, China

⁵ Surveying and Mapping Engineering Institute of Hubei Province, Wuhan 430074, China

* Correspondence: guofeng.wu@szu.edu.cn; Tel.: +86-755-2693-3149

Academic Editor: Richard Henry Moore

Received: 15 May 2016; Accepted: 17 August 2016; Published: 22 August 2016

Abstract: Suspended particulate matter concentration (C_{SPM}) is a key parameter describing case-II water quality. Empirical and semi-empirical models are frequently developed and applied for estimating C_{SPM} values from remote sensing images; however, they are usually region- or season-dependent. This study aimed to develop a Moderate Resolution Imaging Spectroradiometer (MODIS)-based retrieval model of C_{SPM} for Poyang and Dongting Lake together. The 89 C_{SPM} measurements in Poyang and Dongting Lake as well as their corresponding MODIS Terra images were used to calibrate C_{SPM} retrieval models, and the calibration results showed that the exponential models of MODIS red band and red minus shortwave infrared (SWIR) band at 1240 nm both explained about 76% of the variation of C_{SPM} of Poyang and Dongting Lake together. When the two models were applied to the validation datasets, the results indicated that the exponential model of red band obtained more stable C_{SPM} estimations with no bias at a significance level of 0.05 in both lakes. The MODIS red-band-based model achieved acceptable results for estimating C_{SPM} in both Poyang and Dongting Lake, and it provided a foundation for obtaining comparable spatiotemporal information of C_{SPM} , which will be helpful for comparing, understanding, managing, and protecting the two aquatic ecosystems.

Keywords: lake management; water quality; remote sensing; empirical model

1. Introduction

The inland and coastal case-II waters are important for social and economic development, tourism, recreation, and biodiversity conservation, and they are being paid close attention due to the increasing impacts of local or regional social and economic development as well as global environmental change. Suspended particulate matter (SPM) is a primary constituent of case-II water, and it increases water turbidity, reduces water quality, and further affects the whole aquatic ecosystem [1–3]. SPM concentration (C_{SPM}) is a key parameter commonly used to describe water quality [4,5], and its spatiotemporal distributions are useful for monitoring and understanding water quality dynamics and further for managing and protecting aquatic ecosystems.

The spatiotemporal distributions of C_{SPM} for case-II waters are frequently obtained using remote sensing techniques, in which Moderate Resolution Imaging Spectroradiometer (MODIS) images have great potentials for large water bodies due to their advantages of daily coverage, high sensitivity, and cost-free distribution. Many studies have employed MODIS images to estimate the C_{SPM} values of water bodies, such as the Roosevelt, Bartlett, and Pleasant Lakes [6] and Chesapeake Bay [7,8] in the United States; the Pakri Bay in Finland [9]; as well as the Yangtze River [10] and Taihu Lake [11,12] in China (Table 1).

Table 1. Some published regression models of suspended particulate matter concentration (C_{SPM} , $\text{mg}\cdot\text{L}^{-1}$) based on Moderate Resolution Imaging Spectroradiometer (MODIS). R_{rs} is the remote sensing reflectance at the wavelength of λ nm, R^2 is the determination coefficient of calibrated model, and n is the number of sampling. Source: modified based on Wu et al. [13].

Author(s)	Model	R^2	n	C_{SPM} Range	Location
Ody et al. (2016) [14]	$C_{SPM} = 1400 R_{rs}(645)$	0.61	27	3–60	Rhone River, France
Chen et al. (2015) [15]	$\log_{10}(R_{rs}(859))/\log_{10}(R_{rs}(645)) = -0.334 \log_{10}(C_{SPM})^2 + 1.0046 \log_{10}(C_{SPM}) + 0.8251$	0.75	60	5.8–577.2	Etuary of Yangtze River and Xuwen Coral Reef Protection Zone, China
Wu et al. (2014) [16]	$C_{SPM} = 3.04 \exp(20.23 (R_{rs}(645) - R_{rs}(1240)))$	0.68	48	0.1–40.4	Dongting Lake, China
Qiu (2013) [17]	$\log_{10}(C_{SPM}) = 1.932 \exp(0.875 R_{rs}(678)/R_{rs}(551))$	0.95	122	1.9–1896.5	Yellow River Estuary, China
Villar et al. (2013) [18]	$C_{SPM} = 1020 (R_{rs}(859)/R_{rs}(645))^{2.94}$	0.62	282	25–622	Maderia River, Brazil
Long and Pavelsky (2013) [19]	$C_{SPM} = 12.996 \exp(R_{rs}(859)/(0.189R_{rs}(645)))$	0.94	147	3.9–3602	Peace-Athabasca Delta, Canada
Wu et al. (2013) [13]	$C_{SPM} = 0.0365 \exp(63.2 (R_{rs}(645) - R_{rs}(1240)))$	0.76	42	0–141.9	Poyang Lake, China
Feng et al. (2012) [20]	$C_{SPM} = 0.6786 \exp(34.366 (R_{rs}(645) - R_{rs}(\text{nearest}1240)))$	0.87	38	3–200	Poyang Lake, China
Jiang and Liu (2011) [21]	$C_{SPM} = 1365.5 (R_{rs}(470) + R_{rs}(555))^2 - 369.08 (R_{rs}(470) + R_{rs}(555)) + 27.216$	0.81	27	0–40	Poyang Lake, China
Chen et al. (2011) [22]	$\log_{10}(R_{rs}(859))/\log_{10}(R_{rs}(645)) = -0.1325 \log_{10}(C_{SPM})^2 + 0.7429 \log_{10}(C_{SPM}) + 0.6768$	0.86	32	1.29–208	Apalachicola Bay, United States
Zhao et al. (2011) [23]	$C_{SPM} = 2.12 \exp(45.92 R_{rs}(645))$	0.78	63	0–87.8	Mobile Bay Estuary, Alabama
Tarrant et al. (2010) [6]	$C_{SPM} = 0.0213 (R_{rs}(645) - R_{rs}(859)) + 0.232$	0.82	105	0.30–13.4	Roosevelt, Bartlett Pleasant Lake, United States
Zhang et al. (2010) [11]	$\ln(C_{SPM}) = 0.015 (R_{rs}(645)) + 0.003 (R_{rs}(645))^2 - 0.282$	0.87	166	4.32–311.4	Taihu Lake, China
	$\ln(C_{SPM}) = 166.960/(R_{rs}(470) - R_{rs}(645)) - 2.192$	0.79			
	$\ln(C_{SPM}) = -16.997 R_{rs}(470)/R_{rs}(645) + 3.326 (R_{rs}(470)/R_{rs}(645))^2 + 23.681$	0.87			
Wang and Lu (2010) [24]	$\ln(C_{SPM}) = -29.707 (R_{rs}(470) - R_{rs}(645))/(R_{rs}(470) + R_{rs}(645)) + 41.886 (R_{rs}(470) - R_{rs}(645))/(R_{rs}(470) + R_{rs}(645))^2 + 11.358$	0.87			
Wang et al. (2010) [25]	$\ln(C_{SPM}) = 0.262 (R_{rs}(859) - R_{rs}(1240)) + 4.117$	0.78	35	74–881	Lower Yangtze River, China
Wang et al. (2010) [25]	$\log_{10}(C_{SPM}) = 1.5144 \log_{10}(R_{rs}(859))/\log_{10}(R_{rs}(645)) - 0.5755$	0.72	16	1–64	Apalachicola Bay, United States
	$\log_{10}(C_{SPM}) = 0.1497 \exp(1.5859 \log_{10}(R_{rs}(859))/\log_{10}(R_{rs}(645)))$	0.61	11		

Table 1. Cont.

Author(s)	Model	R ²	n	C _{SPM} Range	Location
Jiang et al. (2009) [12]	$\log_{10}(C_{SPM}) = 0.3568 \ln(R_{rs}(859)) + 3.3431$	0.81	56	0–170	Taihu Lake, China
Doxaran et al. (2009) [26]	$C_{SPM} = 12.996 \exp(R_{rs}(859)/(0.189R_{rs}(645)))$	0.89	204	0–2250	Gironde Estuary, France
Wu and Cui (2008) [27]	$C_{SPM} = 86236.23 R_{rs}(645)^3 - 15858.70 R_{rs}(645)^2 + 1005.29 R_{rs}(645) - 15.67$	0.92	42	0–142	Poyang Lake, China
Liu et al. (2006) [28]	$\ln(C_{SPM}) = 2.495 (R_{rs}(645) - R_{rs}(859))/(R_{rs}(645) + R_{rs}(859)) + 1.810$	0.72	41	23.4–61.2	Middle Yangtze River, China
Sipelgas et al. (2006) [9]	$C_{SPM} = 110.3 R_{rs}(645) + 2$	0.58	48	3–10	Pakri Bay, Finland
Hu et al. (2004) [29]	$C_{SPM} = 0.00522 \exp(1002 (R_{rs}(645) - R_{rs}(859)))$	0.90	31	2–11	Tampa Bay, United States

Empirical and semi-empirical models are commonly employed methods for estimating C_{SPM} values since they are simple and easily developed; however they are often region- and time-dependent considering model types (e.g., linear, cubic, and exponential) and estimation accuracies, because they have no strict theoretical foundations and different optical properties appear at different water bodies or even at different time periods [13]. Therefore, the empirical and semi-empirical models developed for a specific water body or season cannot be directly applied to other water bodies or seasons; therefore, the C_{SPM} values retrieved with different models are not comparable, which might limit the simultaneous analysis of water quality of different water bodies [30,31].

Poyang and Dongting Lake are the first and second largest freshwater lakes in China, respectively. So far, several MODIS-based empirical or semi-empirical models have been developed for retrieving the C_{SPM} values in Poyang Lake, including a cubic model of red band [27], a quadratic model of blue plus green band as well as two power models of red band [21], exponential models of red minus shortwave infrared (SWIR) band [13,20], and an exponential model of red band [32]. However, few MODIS-based studies have been carried out to estimate the water quality in Dongting Lake, based on our latest literature review and knowledge; for example, Wu et al. [16] developed an exponential model of MODIS red minus SWIR band at 1240 nm for estimating the C_{SPM} values in this lake.

Poyang and Dongting Lake both connect to the Yangtze River, and they have some similar hydrological characteristics. Thus, it is theoretically and practically meaningful to develop a common water quality retrieval model for Poyang and Dongting Lake in order to compare their water quality properties for lake study and management. The objective of this study was to develop a MODIS-based retrieval model of C_{SPM} for Poyang and Dongting Lake together, which will lay the foundation for obtaining comparable C_{SPM} values from MODIS images and for further comparing the water quality properties of the two lakes.

2. Methods

2.1. Study Area

Poyang Lake (115°47′–116°45′ E, 28°22′–29°45′ N) (Figure 1) receives the water from five rivers (Raohe, Xinjiang, Fuhe, Ganjiang, and Xiushui) and drains into the Yangtze River. The lake has large fluctuant areas from <1000 km² in dry seasons (December–February) to around 4000 km² in flood seasons (July–August) [33,34]. Poyang Lake plays very important roles in local economic and social developments as well as in global ecological conservation, and it is also an internationally important wetland and one of the largest bird conservation areas in the world [35]. SPM is a dominant factor affecting the water quality of Poyang Lake; especially, since 2001 the intensive sand dredging activities have been causing sediments to become resuspended and increase water turbidity [32,36].

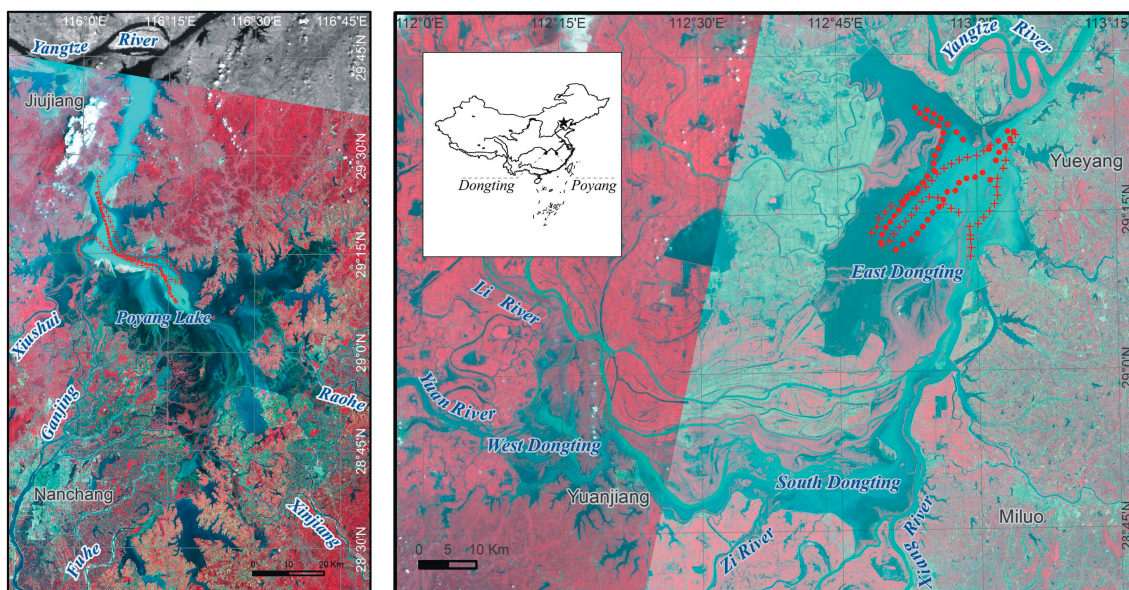


Figure 1. Maps showing the sampling sites in Poyang (circle: 27 September 2007, cross: 31 August 2012) and Dongting (cross: 31 August 2012, circle: 14 June 2013) Lake.

Dongting Lake ($110^{\circ}40'–113^{\circ}10'$ E, $28^{\circ}30'–30^{\circ}20'$ N) (Figure 1) changes from <500 km² in the dry seasons to around 2500 km² in the flood seasons [37], and it includes three parts (East, South and West), of which the East Dongting is the biggest one. The waters of Dongting Lake are mainly from the Xiang, Zi, Yuan, Li, and Yangtze River, flow into the western and southern parts, and drain into the Yangtze through the eastern part. Dongting Lake is also an internationally important wetland with a rich biodiversity [38], and its biggest environmental problem is rapid sedimentation [16,39].

2.2. Fieldwork and C_{SPM} Measurement

Four fieldworks were carried out in 2007, 2012, and 2013 in Poyang and Dongting Lake (Table 2), and a total 197 water samples were collected. In each fieldwork, the sampling work started around 10 a.m. local time when the sunlight and weather condition were relatively steady, the selected sampling sites were distributed from clear to turbid water, and the distance between any two sampling sites was not less than 1.5 km. At each sampling site, a global positioning system receiver (Garmin International, Inc., Olathe, KS, USA) was used to record the location coordinates, and about 1000–1500 mL of surface water was collected from a water depth of around 0–50 cm for C_{SPM} measurement in laboratory [16,27,32].

The C_{SPM} values of water samples were measured in the laboratory according to the investigation criteria about the lakes of China [40] as follows: one 0.45 μm nucleopore membrane filter was first weighed, wetted with distilled water, dried for 1 h at 110 $^{\circ}\text{C}$ in a drying oven, and reweighed after recovering to room temperature in a desiccator. The water sample was then shaken to suspend the sediments, and poured through the membrane filter in a vacuum pump filtration apparatus; the membrane filter was dried for 2 h at 110 $^{\circ}\text{C}$ and reweighed after cooling to room temperature in the desiccator. Finally, the C_{SPM} was calculated by dividing the weight difference of membrane filter before and after filtering by the water sample volume.

Table 2. Description of four fieldworks and their corresponding MODIS images in Poyang and Dongting Lake. Original sampling number is the number of samples collected in the fields, and employed sampling number is the number of samples employed in this study after removing outliers.

Lake	Fieldwork Date	Original Sampling Number	Employed Sampling Number	MODIS Date
Poyang Lake	27 September 2007	42	42	27 September 2007
	31 August 2012	54	48	30 August 2012
Dongting Lake	31 August 2012	48	47	30 August 2012
	14 June 2013	53	48	14 June 2013

2.3. Image Acquisition and Pre-Processing

The Terra satellite, as the flagship Earth Observing Satellite, travels in a circular sun-synchronous polar orbit with the descending node at 10:30 a.m. local time, and the MODIS instrument aboard the Terra satellite observing every point on the Earth every 1–2 days [41]. MOD09GQ and MOD09GA data are the surface reflectance products (Collection 5) derived from MODIS Terra level 1B images using the 6S atmospheric algorithm [42,43], in which several key parameters including geometrical conditions, atmospheric model, aerosol model, and aerosol concentration are inputted to correct the effect of atmospheric gases, aerosols, and thin cirrus clouds [44]. The data provide an estimation of the spectral reflectance as it would be measured at ground level in the absence of atmospheric scattering or absorption. The MOD09GQ product contains two 250 m bands at 645 and 858 nm, and the MOD09GA stores seven 500 m or 1 km bands centred at 645, 858, 470, 555, 1240, 1640, and 2130 nm [45]. Considering the uncertainty of current atmospheric algorithms for case-II waters, the MOD09GQ and MOD09GA images—which have been frequently used by Wang et al. [46], Ayana et al. [47], Chen et al. [15], Doxaran et al. [26], and Alcântara et al. [48]—were employed in this study directly.

The MOD09GQ and MOD09GA images corresponding to the four fieldworks in this study (Table 2) and on 1 August 2013 were downloaded from the Land Processes Distributed Active Archive Centre (LP DAAC) [49]. The pre-processes used in Cui et al. [32] and Wu et al. [16] were employed in this study as follows: all downloaded images were projected into WGS 84/UTM (zone 49N for Dongting Lake, and zone 50N for Poyang Lake) using nearest-neighbor resampling method to preserve original reflectance value; for each image, a sub-image covering the study area was cut from the original image, and the land areas and small water bodies were removed using a binary mask created by visually interpreting its unsupervised classification image.

2.4. Model Development

Four sampling points with high reflectance at 1240 nm (>10%) and two sampling points with high C_{SPM} value (>160 mg·L⁻¹) on 31 August 2012 were removed for Poyang Lake; for Dongting Lake, one sampling point on 31 August 2012 was removed due to its high reflectance at 1240 nm (>40%), and four sampling points close to emergent plants (<1 km) with high reflectance at 1240 nm (>10%) and one point with high C_{SPM} value (63.2 mg·L⁻¹) on 14 June 2013 were also removed; thus, a total of 185 sampling points (90 for Poyang and 95 for Dongting) were kept for model development in this study (Table 2). The remaining C_{SPM} measurements of each fieldwork were statistically described respectively using STATISTICA software package [50].

With the support of STATISTICA, the model calibration process used by Wu et al. [16] was employed to develop the retrieval models of C_{SPM} for Poyang and Dongting Lake, respectively, as follows: (1) the 42 C_{SPM} measurements on 27 September 2007 in Poyang Lake and 47 on 31 August 2012 in Dongting Lake, as well as their corresponding MODIS images, were applied to calibrate the linear, quadratic, and exponential models of C_{SPM} against a single 250 m red and near-infrared (NIR) band, as well as the combinations listed in Table 1 (such as red-NIR, NIR/red, and (red-NIR)/(red + NIR)), respectively, using the least-squares technique; (2) the abovementioned

models were calibrated again using the MODIS red or NIR band minus SWIR band at 1240 or 1640 nm, respectively, since adopting the difference between MODIS red or NIR band and SWIR band at 1240 or 1640 nm might refine the atmospheric correction results for turbid waters and thus improve the retrieval models [20,51]. In order to develop common models for Poyang and Dongting Lake, considering at certain levels the spatial and temporal extendibility of the developed models, the datasets of these two lakes (42 C_{SPM} measurements on 27 September 2007 in Poyang Lake and 47 on 31 August 2012 in Dongting Lake) were put together, and the aforementioned calibration process was repeated. By comparing the determination coefficients (R^2) and estimated standard errors (SE) of all calibrated models as well as model complexity, the two best-fitting models were selected for Poyang and Dongting Lake as well as their combination, respectively.

The 48 C_{SPM} measurements on 31 August 2012 in Poyang Lake and 48 on 14 June 2013 in Dongting Lake with their corresponding MODIS images were used to validate the above selected two models for Poyang and Dongting Lake together, respectively. Each model was applied to estimate the C_{SPM} values at sampling sites from the MODIS images. The correlation coefficient (r) between the measured and estimated C_{SPM} values as well as the root mean square error ($RMSE$) and relative root mean square error ($RRMSE$) of estimation were calculated to assess model performances. Besides, the null hypotheses that the slope and intercept of the linear regression line between the measured and estimated C_{SPM} values were equal to 1 and 0, respectively, were tested to evaluate the model bias.

2.5. Model Application

Considering the aforementioned model validation results, the most stable model was chosen and applied to the MODIS Terra images captured on 1 August 2013 to retrieve the C_{SPM} values of Poyang and Dongting Lake, and their spatial distribution and driving factors were compared and analyzed briefly.

3. Results

3.1. C_{SPM} Measurement

The statistics of remaining C_{SPM} measurements of four fieldworks in Poyang and Dongting Lake are shown in Table 3. The C_{SPM} values do not show a statistically significant difference at a significance level of 0.05 between the two fieldworks for each lake (z -test for mean difference: mean C_{SPM} in Poyang: $38.2 \pm 42.0 \text{ mg}\cdot\text{L}^{-1}$ on 27 September 2007 and $42.3 \pm 43.3 \text{ mg}\cdot\text{L}^{-1}$ on 31 August 2012, $z = -0.46$, $p = 0.65$; mean C_{SPM} in Dongting: $12.6 \pm 13.8 \text{ mg}\cdot\text{L}^{-1}$ on 31 August 2012 and $10.8 \pm 10.4 \text{ mg}\cdot\text{L}^{-1}$ on 14 June 2013, $z = 0.69$, $p = 0.49$), and the variations of C_{SPM} values were similar for the two lakes (variation coefficient = 96.2%–110.1%); however, as a whole, the C_{SPM} value in Poyang Lake was higher than that in Dongting Lake.

Table 3. Statistics describing the variation of suspended particulate matter concentrations (C_{SPM} , $\text{mg}\cdot\text{L}^{-1}$) of the water samples collected in Poyang ($n = 90$) and Dongting ($n = 95$) Lake.

C_{SPM}	Poyang Lake		Dongting Lake	
	27 September 2007 ($n = 42$)	31 August 2012 ($n = 48$)	31 August 2012 ($n = 47$)	14 June 2013 ($n = 48$)
Minimum	0.0	0.0	0.0	0.7
Maximum	141.9	144.0	40.4	44.8
Mean	38.2	42.3	12.6	10.8
Standard deviation	42.0	43.3	13.8	10.4
Variation coefficient	110.1	102.3	109.6	96.2

3.2. Model Development

Based on the 42 C_{SPM} measurements in Poyang Lake and 47 in Dongting Lake, as well as their corresponding MODIS images, model calibration results showed that the red band and the red minus SWIR band at 1240 nm obtained the best fit among all tested models for Poyang and Dongting Lake as well as the two lakes together, respectively (Figure 2). The exponential model of red band explained 71% ($SE = 23 \text{ mg}\cdot\text{L}^{-1}$) of the variation of C_{SPM} for Poyang and 71% ($SE = 7 \text{ mg}\cdot\text{L}^{-1}$) for Dongting Lake; the exponential model of red band for Poyang and Dongting Lake together slightly improved fitting accuracy compared with that for each lake alone, considering R^2 value ($= 0.76$) (Figure 2A). The red minus SWIR band at 1240 nm could barely improve the model accuracy for Dongting Lake, and its exponential model explained 72% ($SE = 6 \text{ mg}\cdot\text{L}^{-1}$) of the variation of C_{SPM} ; however, it obtained a higher fitting accuracy than the single red band for Poyang Lake ($R^2 = 0.75$, $SE = 21 \text{ mg}\cdot\text{L}^{-1}$). The exponential model of red minus SWIR band at 1240 nm for Poyang and Dongting Lake together also slightly improved the fitting accuracy than that for each lake alone, considering R^2 value ($= 0.76$) (Figure 2B).

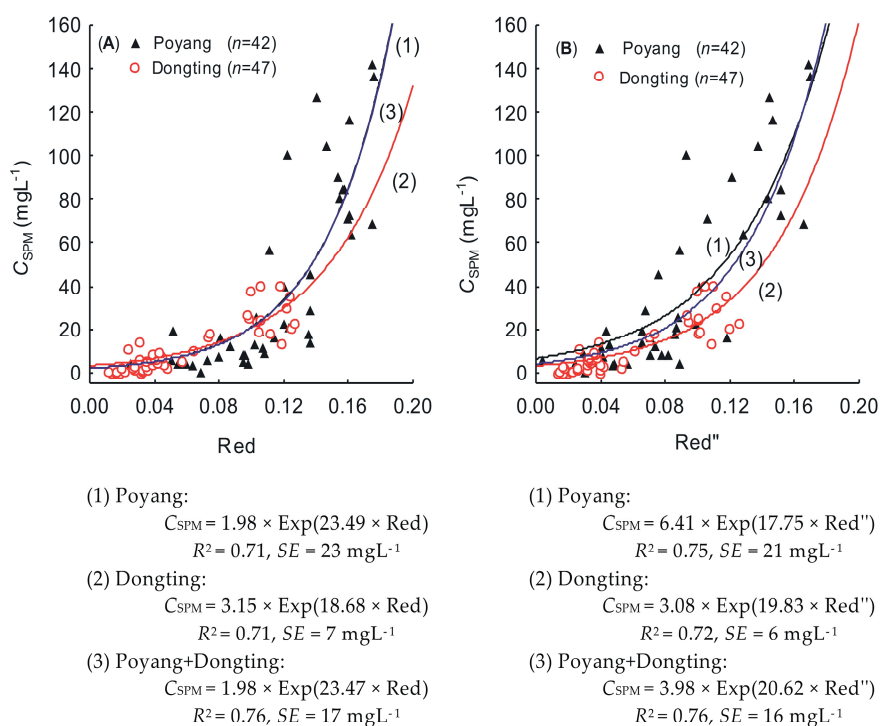


Figure 2. Scattering plots showing the regression models of suspended particulate matter concentration (C_{SPM} , $\text{mg}\cdot\text{L}^{-1}$) against the red band (Red) (A) and the red minus shortwave infrared (SWIR) band at 1240 nm (Red'') (B) of MODIS Terra images for Poyang ($n = 42$), Dongting ($n = 47$) Lake and their combination ($n = 89$).

The exponential models of red band and the red minus SWIR band at 1240 nm for Poyang and Dongting Lake together were applied to the validation datasets to estimate their C_{SPM} values, respectively, and the results of comparing the measured and estimated C_{SPM} values are shown in Figure 3. There existed significantly strong correlations between the measured and estimated C_{SPM} values for both models and both lakes at a significance level of 0.05 ($r = 0.80\text{--}0.87$, $p < 0.05$). The model of red minus SWIR band at 1240 nm ($r = 0.87$, $RMSE = 22 \text{ mg}\cdot\text{L}^{-1}$, $RRMSE = 54\%$) obtained a bit higher estimation accuracy than that of red band ($r = 0.81$, $RMSE = 26 \text{ mg}\cdot\text{L}^{-1}$, $RRMSE = 64\%$) for Poyang Lake, while the results of null hypothesis tests of intercept being 0 and slope being 1 for the regression line between the measured and estimated C_{SPM} values indicated that the intercept

and slope were not significantly different from 0 and 1 for both models at a significance level of 0.05 (Table 4). However, for Dongting Lake, the model of red band ($r = 0.85$, $RMSE = 7 \text{ mg}\cdot\text{L}^{-1}$, $RRMSE = 55\%$) obtained higher estimation accuracy than that of red minus SWIR band at 1240 nm ($r = 0.80$, $RMSE = 9 \text{ mg}\cdot\text{L}^{-1}$, $RRMSE = 76\%$), while an estimation bias was observed for the model of red minus SWIR band at 1240 nm (Table 4), as the result of null hypothesis test of slope being one for the regression line between the measured and estimated C_{SPM} values showed that the slope was significantly different from one at a significance level of 0.05 ($b = 0.816$, $p = 0.042$), which suggests an overestimation of the measured C_{SPM} for this model (Figure 3B). Thus, the exponential model of MODIS red band obtained the best stable result for estimating the C_{SPM} values in both Poyang and Dongting Lake.

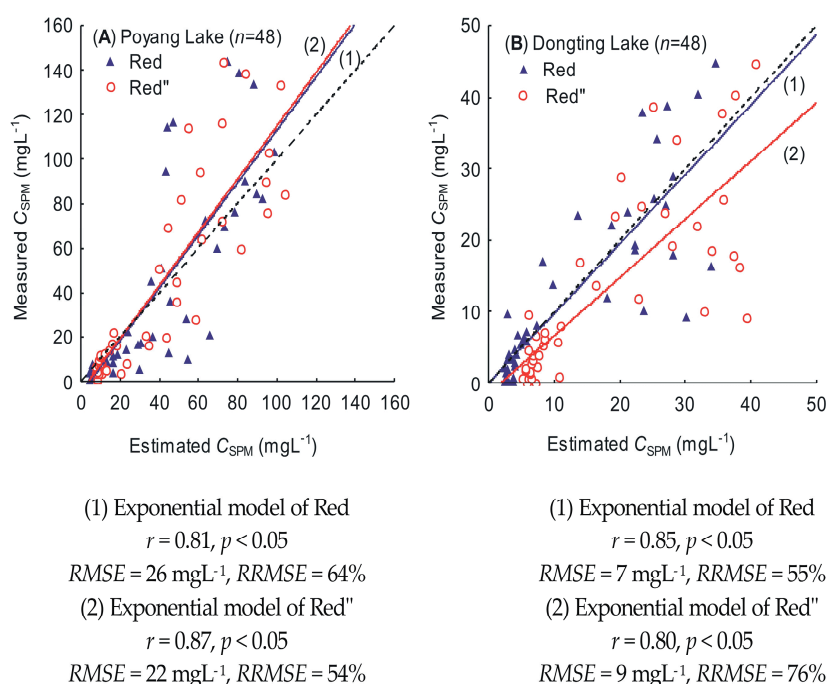


Figure 3. Scattering plots showing the measured suspended particulate matter concentration (C_{SPM} , $\text{mg}\cdot\text{L}^{-1}$) against the estimated one using the exponential models of the red band (Red) as well as the red minus SWIR band at 1240 nm (Red'') of MODIS Terra images for Poyang ($n = 48$) (A) and Dongting ($n = 48$) (B) Lake. The solid line is the regression line between measured and estimated values, the dashed line is 1:1 line, r is the correlation coefficient between measured and estimated values, p is the probability of significance testing for correlation coefficient, and $RMSE$ and $RRMSE$ are the root mean square error ($\text{mg}\cdot\text{L}^{-1}$) and relative root mean square error (%) of estimation, respectively.

Table 4. Null hypothesis tests of the intercept (a) = 0 and slope (b) = 1 of the regression line between the measured and estimated suspended particulate matter concentrations (C_{SPM} , $\text{mg}\cdot\text{L}^{-1}$) of the water samples collected in Poyang ($n = 48$) and Dongting ($n = 48$) Lake. SE is standard error, t is the value of Student's t -test, p is the probability in null hypothesis significance testing and the bold p value suggests that the null hypothesis test is statistically significant at a significance level of 0.05. (A)-(B) correspond to the model number used in Figure 3.

	Intercept (a)			Slope (b)		
	$a \pm SE$	t	p	$b \pm SE$	t	p
(A)-(1)	-5.470 ± 6.470	-0.845	0.403	1.186 ± 0.132	1.405	0.160
(A)-(2)	-4.660 ± 5.019	-0.928	0.358	1.196 ± 0.101	1.936	0.053
(B)-(1)	-0.029 ± 1.447	-0.020	0.984	0.975 ± 0.089	-0.284	0.776
(B)-(2)	-1.554 ± 1.840	-0.844	0.403	0.816 ± 0.090	-2.035	0.042

3.3. Model Application

The most stable model with MODIS red band ($C_{SPM} = 1.98 \times \text{Exp}(23.47 \times \text{Red})$, $R^2 = 0.76$, $SE = 17 \text{ mg}\cdot\text{L}^{-1}$) was applied to the MODIS Terra images captured on 1 August 2013 to retrieve the C_{SPM} values of Poyang and Dongting Lake (Figure 4). In general, the C_{SPM} values of Poyang Lake were higher than those in Dongting Lake. A conspicuous turbid region (C_{SPM} values were close to $200 \text{ mg}\cdot\text{L}^{-1}$) was observed from the southeast to the north in Poyang Lake, which was caused by the dredging activities and their related vessel shipping in the southern and middle Poyang Lake [52]. The C_{SPM} values in the east were higher than those in the southwest of Poyang Lake, which could be explained by the fact that the shallower water in the east made the sediments suspended and increased C_{SPM} values. The general spatial distribution pattern of C_{SPM} and its driving factors in Dongting Lake were provided by Wu et al. [16] as follows. The C_{SPM} values of South Dongting were higher than those of West Dongting, which could be explained by the fact that the C_{SPM} values of South Dongting were affected by the turbid inflow of Li River (Figure 1). A small turbid region was observed at the western part of East Dongting (region 1 in Figure 4), which was also induced by the turbid river inflow (Figure 1). A large area with high C_{SPM} values (about $40\text{--}60 \text{ mg}\cdot\text{L}^{-1}$) appeared at the eastern part of East Dongting (region 2 in Figure 4). Dredging activities were also observed at East Dongting Lake (region 3 in Figure 4) from our fieldworks, and they and their related vessel shipping increased the C_{SPM} values at dredging regions and downstream of them. Thus, the turbid inflow from the South Dongting and dredging at East Dongting Lake together could explain the high C_{SPM} values observed at the eastern part of East Dongting Lake.

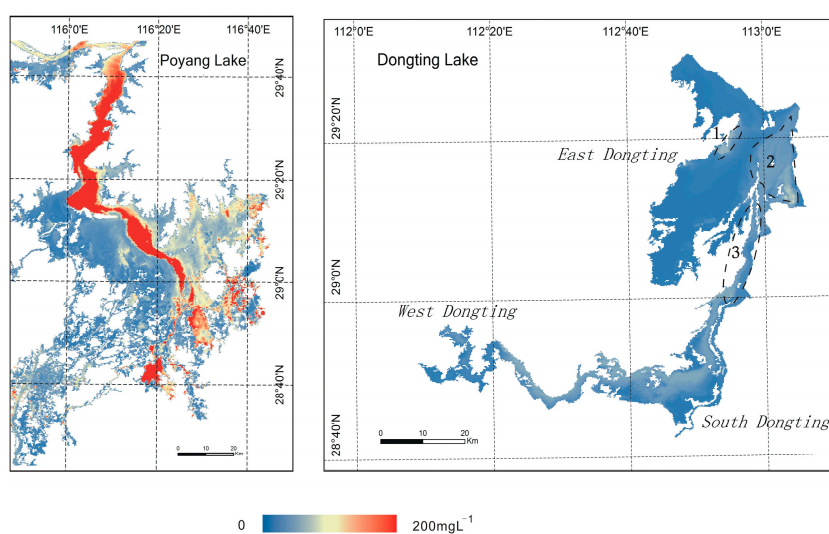


Figure 4. Suspended particulate matter concentrations retrieved from the MODIS Terra images captured on 1 August 2013 for Poyang and Dongting Lake. Dashed circles labelled with numbers indicated the different regions in Dongting Lake.

4. Discussion

It is important to ensure the concurrence of satellite image overpass and fieldwork in order to develop remote-sensing-based water quality parameter retrieval models, because a large time difference between them usually reduces model accuracy due to the water quality parameter change, especially for a very dynamic waterbody. In our study, the MODIS image on 30 August 2012 and the C_{SPM} values measured on 31 August 2012 were involved in model development process, which might influence model development to some extent. However, since there was no rainfall or large changes in wind speed and water level during these two days, we considered that this effect should be very weak.

For the MODIS red and NIR bands, one image pixel covers an area of about $250 \text{ by } 250 \text{ m}^2$, while its corresponding C_{SPM} value for model development is generally derived from the water sample

collected at one site. Thus, a scale gap exists between image pixel and C_{SPM} measurement, which has a significant impact on the development of water quality retrieval models. During our fieldworks, sand dredging activities occurred in both lakes, which cause sediments to become resuspended and caused C_{SPM} values anomalies in some regions. Such anomalous C_{SPM} values and scale gap problem could explain why two samples with high C_{SPM} values at the turbid region in Poyang Lake and one sample in Dongting Lake were removed, respectively, from our study. Besides, we found that four sampling points in Poyang Lake were close to the lake shores and five in Dongting Lake were close to the plant regions, and their corresponding MODIS reflectance values at 1240 nm were too high, which indicated that these image pixels might partly cover lake shores and plant regions, because the reflectance values of pure water pixels at 1240 nm are nearly zero. Thus, we removed these nine samples to avoid the influence of mixed pixels on model accuracy.

Many studies reported that the empirical and semi-empirical models for water quality retrievals were often region- and time-dependent, since they have no strict theoretical foundations and the optical properties are often different at different water bodies or even at different seasons. Developing a model for simultaneously estimating water quality parameters of different lakes could thus be meaningful. The suspended particulate inorganic matter (suspended sediment) is dominant within the water constituents of Poyang Lake [53], and the chlorophyll occupied a very low proportion within the C_{SPM} value in Dongting Lake (mean chlorophyll a concentration = $2.8 \mu\text{g}\cdot\text{L}^{-1}$ on 31 August 2012, $n = 48$, unpublished result). We considered that the similar water constituent structures of the two lakes might explain why a common model could be developed for the both lakes. The C_{SPM} retrieval model developed in this study might be applicable to other water bodies with similar optical properties as that in Poyang and Dongting, however, a careful model validation should be carried out first.

In this study, we found that the red band of the MODIS image obtained the best result for estimating the C_{SPM} values in Poyang and Dongting Lake (Figures 2 and 3), and such a result is consistent with that of many water bodies (Table 1). The absorption and backscattering characteristics of main water constituents (including phytoplankton, suspended sediment, yellow substance, and water itself) may explain why the MODIS red band has potential for the C_{SPM} estimations in case-II waters, which has been discussed in many studies [1,30,54–56]. Repeatedly, the absorption coefficients of main water constituents decrease with the increasing wavelength and are close to zero in red and near infrared regions, especially for the water bodies with low phytoplankton concentration like Poyang and Dongting Lake. Therefore, the backscattering coefficients of phytoplankton and yellow substance can also be neglected over these regions, and thus the water-leaving radiances, which are captured by remote sensing sensor and employed for estimating water quality parameters, are dominated by the backscattering coefficient of suspended sediment in the red or near-infrared regions [16,32].

The exponential model of MODIS red band explained 76% of the C_{SPM} variation in Poyang and Dongting Lake together (Figure 2). Considering that the model is a common model for two lakes, such model fitting accuracy is moderate and acceptable compared with that in other water bodies such as Rhone River, Maderia River, Taihu Lake, and Tampa Bay in Table 1 ($R^2 = 0.58\text{--}0.95$). Many factors may affect model fitting accuracy. Wu et al. [13], based on an analysis of 28 MODIS-based C_{SPM} retrieval models, considered that the C_{SPM} value range and sampling number might not be the most important factors affecting model fitting accuracy; thus the C_{SPM} value range ($0\text{--}144.0 \text{ mg}\cdot\text{L}^{-1}$) and sampling number (89 sampling points) employed in this study were large enough. The C_{SPM} measurements and their corresponding MODIS images from two lakes might decrease estimation accuracy in this study, because different water bodies have different water constituents and different inherent optical properties; however, we did not find a decreased model-fitting accuracy when putting the datasets of Poyang and Dongting Lake together (Figure 2). There exists a scale gap between image pixel and C_{SPM} measurement, and it is generally assumed that the C_{SPM} value within a pixel is homogeneous; however, such an assumption is often not valid [16], especially for Poyang and Dongting Lake because of the dredging impacts on C_{SPM} distribution in some regions. We considered

that the scale gap between image pixel and C_{SPM} measurement and the large heterogeneity of C_{SPM} value for some pixels could be the most important factors affecting model fitting accuracy.

We also found that, compared with the red band, the red minus SWIR band at 1240 nm did not produce much better fitting results for Dongting Lake as well as for Dongting and Poyang Lake together (Figure 2). Such a result indicated that using the SWIR values at 1240 nm to remove atmospheric effects might not always improve the model-fitting accuracy in all cases. And it showed instability and uncertainty. Such a result might be explained by the fact that (1) the water reflectance at 1240 nm was not always zero [57] due to the changing water constituent structure; and (2) the reflectance at 1240 nm was also not stable and showed some uncertainty because of the lower sensor band signal-to-noise ratio values of the MODIS SWIR bands [58]. Several atmospheric correction methods have been developed for case-II waters [20,58–60]; although they also showed uncertainty or even failed in very turbid waters, they or other potential atmospheric methods for the two lakes together should be further explored in order to accurately derive the comparable results of water quality.

Poyang and Dongting Lake are the only remaining large Yangtze-connected lakes at its middle and lower reaches, and they have some similar hydrological characteristics, such as same flooding season and large water level fluctuation. However, we observed a large difference on C_{SPM} between these two lakes (Table 3 and Figure 4), which might be caused by natural or human factors. The dredging activities, which resuspended sediments and increased C_{SPM} , were both found in Poyang and Dongting Lake [20,52,61], and we considered that dredging might explain the large difference on C_{SPM} in the two lakes. The dredging-related C_{SPM} variation is impacted by dredging manner and intensity, water depth, or the size of sediments; however, at present, we do not know which factor(s) might be dominant in causing the large C_{SPM} difference between the two lakes due to limited relevant knowledge.

Poyang and Dongting Lake both play very important roles in local social and economic developments as well as in global ecological conservation; for example, they are the internationally important wetlands and large bird conservation areas in the world. The two lakes are also facing similar water quality degradation due to global climate change and regional or local human activities, such as the impacts of Three Gorges Project and sand dredging activities on water quality and sediment exchanges. Obtaining the comparable spatiotemporal information of C_{SPM} in the two lakes is prerequisite for comparing their water quality and sediment dynamics, analyzing their driving factors, and further improving lake management. The model developed in this study provided a foundation for obtaining the comparable spatiotemporal information of C_{SPM} in Poyang and Dongting Lake together.

5. Conclusions

It is theoretically and practically meaningful to develop water quality retrieval models for different lakes together in order to compare their water quality properties. A C_{SPM} retrieval model using the 250 m red band of MODIS image was developed for Poyang and Dongting Lake ($C_{SPM} = 1.98 \times \text{Exp}(23.47 \times \text{Red})$, $R^2 = 0.76$, $SE = 17 \text{ mg}\cdot\text{L}^{-1}$) together, and it obtained an acceptable result in estimating C_{SPM} values. The developed model provides a foundation for obtaining the comparable spatiotemporal information of C_{SPM} , which would be helpful for comparing, understanding, managing, and protecting Poyang and Dongting aquatic ecosystems.

Acknowledgments: This study was supported by the Scientific Research Foundation for Newly High-End Talents of Shenzhen University, the Basic Research Program of Shenzhen Science and Technology Innovation Committee (No. JCYJ20151117105543692).

Author Contributions: Fangyuan Chen and Guofeng Wu conceived and designed the experiments; Guofeng Wu analyzed the data and helped to outline the manuscript structure; Junjie Wang, Junjun He and Yihan Wang contributed equally by conducting fieldwork and laboratory analysis; Fangyuan Chen prepared the draft of the manuscript.

Conflicts of Interest: The authors declare no conflict of interest.

References

1. Kirk, J.T.O. *Light and Photosynthesis in Aquatic Ecosystems*; Cambridge University Press: New York, NY, USA, 1994; p. 400.
2. Giardino, C.; Oggioni, A.; Bresciani, M.; Yan, H.M. Remote Sensing of Suspended Particulate Matter in Himalayan Lakes A Case Study of Alpine Lakes in the Mount Everest Region. *Mt. Res. Dev.* **2010**, *30*, 157–168. [[CrossRef](#)]
3. Xing, Q.G.; Lou, M.J.; Chen, C.Q.; Shi, P. Using in situ and Satellite Hyperspectral Data to Estimate the Surface Suspended Sediments Concentrations in the Pearl River Estuary. *IEEE J. Sel. Top. Appl. Earth Obs. Remote Sens.* **2013**, *6*, 731–738. [[CrossRef](#)]
4. Pozdnyakov, D.; Shuchman, R.; Korosov, A.; Hatt, C. Operational algorithm for the retrieval of water quality in the Great Lakes. *Remote Sens. Environ.* **2005**, *97*, 352–370. [[CrossRef](#)]
5. Uddin, S.; Al-Ghadban, A.N.; Gevao, B.; Al-Shamroukh, D.; Al-Khabbaz, A. Estimation of suspended particulate matter in Gulf using MODIS data. *Aquat. Ecosyst. Health Manag.* **2012**, *15*, 41–44.
6. Tarrant, P.E.; Amacher, J.A.; Neuer, S. Assessing the potential of Medium-Resolution Imaging Spectrometer (MERIS) and Moderate-Resolution Imaging Spectroradiometer (MODIS) data for monitoring total suspended matter in small and intermediate sized lakes and reservoirs. *Water Resour. Res.* **2010**, *46*. [[CrossRef](#)]
7. Ondrusek, M.; Stengel, E.; Kinkade, C.S.; Vogel, R.L.; Keegstra, P.; Hunter, C.; Kim, C. The development of a new optical total suspended matter algorithm for the Chesapeake Bay. *Remote Sens. Environ.* **2012**, *119*, 243–254. [[CrossRef](#)]
8. Son, S.; Wang, M. Water properties in Chesapeake Bay from MODIS-Aqua measurements. *Remote Sens. Environ.* **2012**, *123*, 163–174. [[CrossRef](#)]
9. Sipelgas, L.; Raudsepp, U.; Kouts, T. Operational monitoring of suspended matter distribution using MODIS images and numerical modelling. *Adv. Space Res.* **2006**, *38*, 2182–2188. [[CrossRef](#)]
10. Zhang, Z.; He, G.; Wang, X. A practical DOS model-based atmospheric correction algorithm. *Int. J. Remote Sens.* **2010**, *31*, 2837–2852. [[CrossRef](#)]
11. Zhang, Y.; Lin, S.; Liu, J.; Qian, X.; Ge, Y. Time-series MODIS image-based retrieval and distribution analysis of total suspended matter concentrations in Lake Taihu (China). *Int. J. Environ. Res. Public Health* **2010**, *7*, 3545–3560. [[CrossRef](#)] [[PubMed](#)]
12. Jiang, X.W.; Tang, J.W.; Zhang, M.W.; Ma, R.H.; Ding, J. Application of MODIS data in monitoring suspended sediment of Taihu Lake, China. *Chin. J. Oceanol. Limnol.* **2009**, *27*, 614–620. [[CrossRef](#)]
13. Wu, G.; Cui, L.; He, J.; Duan, H.; Fei, T.; Liu, Y. Comparison of MODIS-based models for retrieving suspended particulate matter concentrations in Poyang Lake, China. *Int. J. Appl. Earth Obs. Geoinform.* **2013**, *24*, 63–72. [[CrossRef](#)]
14. Ody, A.; Doxaran, D.; Vanhellemont, Q.; Nechad, B.; Novoa, S.; Many, G.; Bourrin, F.; Verney, R.; Pairaud, I.; Gentili, B. Potential of High Spatial and Temporal Ocean Color Satellite Data to Study the Dynamics of Suspended Particles in a Micro-Tidal River Plume. *Remote Sens.* **2016**, *8*, 245. [[CrossRef](#)]
15. Chen, S.; Han, L.; Chen, X.; Li, D.; Sun, L.; Li, Y. Estimating wide range Total Suspended Solids concentrations from MODIS 250-m imageries: An improved method. *ISPRS J. Photogramm. Remote Sens.* **2015**, *99*, 58–69. [[CrossRef](#)]
16. Wu, G.; Liu, L.; Chen, F.; Fei, T. Developing MODIS-based retrieval models of suspended particulate matter concentration in Dongting Lake, China. *Int. J. Appl. Earth Obs. Geoinform.* **2014**, *32*, 46–53. [[CrossRef](#)]
17. Qiu, Z.F. A simple optical model to estimate suspended particulate matter in Yellow River Estuary. *Opt. Express* **2013**, *21*, 27891–27904. [[CrossRef](#)] [[PubMed](#)]
18. Espinoza Villar, R.; Martinez, J.-M.; Le Texier, M.; Guyot, J.-L.; Fraizy, P.; Meneses, P.R.; Oliveira, E.D. A study of sediment transport in the Madeira River, Brazil, using MODIS remote-sensing images. *J. South Am. Earth Sci.* **2013**, *44*, 45–54. [[CrossRef](#)]
19. Long, C.M.; Pavelsky, T.M. Remote sensing of suspended sediment concentration and hydrologic connectivity in a complex wetland environment. *Remote Sens. Environ.* **2013**, *129*, 197–209. [[CrossRef](#)]
20. Feng, L.; Hu, C.; Chen, X.; Tian, L.; Chen, L. Human induced turbidity changes in Poyang Lake between 2000 and 2010: Observations from MODIS. *J. Geophys. Res.* **2012**, *117*. [[CrossRef](#)]
21. Jiang, H.; Liu, Y. Monitoring of TSS concentration in Poyang Lake based on MODIS data. *Yangtze River* **2011**, *42*, 87–90. (In Chinese)

22. Chen, S.; Huang, W.; Chen, W.; Chen, X. An enhanced MODIS remote sensing model for detecting rainfall effects on sediment plume in the coastal waters of Apalachicola Bay. *Mar. Environ. Res.* **2011**, *72*, 265–272. [[CrossRef](#)] [[PubMed](#)]
23. Zhao, H.H.; Chen, Q.; Walker, N.D.; Zheng, Q.A.; MacIntyre, H.L. A study of sediment transport in a shallow estuary using MODIS imagery and particle tracking simulation. *Int. J. Remote Sens.* **2011**, *32*, 6653–6671. [[CrossRef](#)]
24. Wang, J.J.; Lu, X.X. Estimation of suspended sediment concentrations using Terra MODIS: An example from the Lower Yangtze River, China. *Sci. Total Environ.* **2010**, *408*, 1131–1138. [[CrossRef](#)] [[PubMed](#)]
25. Wang, H.; Hladik, C.M.; Huang, W.; Milla, K.; Edmiston, L.; Harwell, M.A.; Schalles, J.F. Detecting the spatial and temporal variability of chlorophyll—A concentration and total suspended solids in Apalachicola Bay, Florida using MODIS imagery. *Int. J. Remote Sens.* **2010**, *31*, 439–453. [[CrossRef](#)]
26. Doxaran, D.; Froidefond, J.-M.; Castaing, P.; Babin, M. Dynamics of the turbidity maximum zone in a macrotidal estuary (the Gironde, France): Observations from field and MODIS satellite data. *Estuar. Coast. Shelf Sci.* **2009**, *81*, 321–332. [[CrossRef](#)]
27. Wu, G.; Cui, L. Time-series MODIS images-based retrieval and change analysis of suspended sediment concentration during flood period in Poyang Lake. *J. Lake Sci.* **2008**, *28*, 6113–6120. (In Chinese)
28. Liu, C.-D.; He, B.-Y.; Li, M.-T.; Ren, X.-Y. Quantitative modeling of suspended sediment in middle Changjiang River from modis. *Chin. Geogr. Sci.* **2006**, *16*, 79–82. [[CrossRef](#)]
29. Hu, C.; Chen, Z.; Clayton, T.D.; Swarzenski, P.; Brock, J.C.; Muller-Karger, F.E. Assessment of estuarine water-quality indicators using MODIS medium-resolution bands: Initial results from Tampa Bay, FL. *Remote Sens. Environ.* **2004**, *93*, 423–441. [[CrossRef](#)]
30. Ma, R.; Duan, H.; Tang, J.; Chen, Z. *Remote Sensing of Lake Water Environment*; Science Press: Beijing, China, 2010; p. 536. (In Chinese)
31. Giardino, C.; Brando, V.E.; Dekker, A.G.; Strombeck, N.; Candiani, G. Assessment of water quality in Lake Garda (Italy) using Hyperion. *Remote Sens. Environ.* **2007**, *109*, 183–195. [[CrossRef](#)]
32. Cui, L.; Qiu, Y.; Fei, T.; Liu, Y.; Wu, G. Using remotely sensed suspended sediment concentration variation to improve management of Poyang Lake, China. *Lake Reserv. Manag.* **2013**, *29*, 47–60. [[CrossRef](#)]
33. Xu, D.; Xiong, M.; Zhang, J. Analysis on hydrologic characteristics of Poyang Lake. *Yangtze River* **2001**, *32*, 21–27.
34. Shankman, D.; Keim, B.D.; Song, J. Flood frequency in China's Poyang lake region: Trends and teleconnections. *Int. J. Climatol.* **2006**, *26*, 1255–1266. [[CrossRef](#)]
35. Wu, Y.; Ji, W. *Study on Jiangxi Poyang Lake National Nature Reserve*; Forest Publishing House: Beijing, China, 2002; p. 231.
36. Wu, G.; De Leeuw, J.; Skidmore, A.K.; Prins, H.H.H.; Liu, Y. Concurrent monitoring of vessels and water turbidity enhances the strength of evidence in remotely sensed dredging impact assessment. *Water Res.* **2007**, *41*, 3271–3280. [[CrossRef](#)] [[PubMed](#)]
37. Huang, S.F.; Li, J.G.; Xu, M. Water surface variations monitoring and flood hazard analysis in Dongting Lake area using long-term Terra/MODIS data time series. *Nat. Hazards* **2012**, *62*, 93–100. [[CrossRef](#)]
38. Wang, Y.X.; Cheng, S.; Ju, H.B.; Zhang, H.Q.; Jiang, D.; Zhuang, D.F. Evaluating sustainability of wetland system: A case study in East Dongting Lake Area, China. *Afr. J. Agric. Res.* **2011**, *6*, 6167–6176.
39. World Lake Database. Available online: http://wldb.ilec.or.jp/data/databook_html/asi/asi-11.html (accessed on 27 April 2016).
40. Huang, X. *Eco-Investigation, Observation and Analysis of Lakes*; Standard Press of China: Beijing, China, 1999. (In Chinese)
41. NASA. TERRA The EOS Flagship. Available online: <http://terra.nasa.gov/about> (accessed on 22 July 2016).
42. Kotchenova, S.Y.; Vermote, E.F.; Matarrese, R.; Klemm, J.F.J. Validation of a vector version of the 6S radiative transfer code for atmospheric correction of satellite data. Part I: Path radiance. *Appl. Opt.* **2006**, *45*, 6762–6774. [[CrossRef](#)] [[PubMed](#)]
43. Kotchenova, S.Y.; Vermote, E.F. Validation of a vector version of the 6S radiative transfer code for atmospheric correction of satellite data. Part II. Homogeneous Lambertian and anisotropic surfaces. *Appl. Opt.* **2007**, *46*, 4455–4464. [[CrossRef](#)] [[PubMed](#)]

44. Vermote, E.F.; Saleous, N. Operational Atmospheric Correction of MODIS Visible to Middle Infrared Land Surface Data in the Case of an Infinite Lambertian Target. In *Earth Science Satellite Remote Sensing: Vol. 1: Science and Instruments*; Qu, J.J., Gao, W., Kafatos, M., Murphy, R.E., Salomonson, V.V., Eds.; Springer Berlin Heidelberg: Berlin/Heidelberg, Germany, 2006; pp. 123–153.
45. USGS. LPDAAC MODIS Products Table. Available online: https://lpdaac.usgs.gov/dataset_discovery/modis/modis_products_table (accessed on 27 April 2016).
46. Wang, J.L.; Zhang, Y.J.; Yang, F.; Cao, X.M.; Bai, Z.Q.; Zhu, J.X.; Chen, E.Y.; Li, Y.F.; Ran, Y.Y. Spatial and temporal variations of chlorophyll—A concentration from 2009 to 2012 in Poyang Lake, China. *Environ. Earth Sci.* **2015**, *73*, 4063–4075. [[CrossRef](#)]
47. Ayana, E.K.; Worqlul, A.W.; Steenhuis, T.S. Evaluation of stream water quality data generated from MODIS images in modeling total suspended solid emission to a freshwater lake. *Sci. Total Environ.* **2015**, *523*, 170–177. [[CrossRef](#)] [[PubMed](#)]
48. Alcântara, E.; Barbosa, C.; Stech, J.; Novo, E.; Shimabukuro, Y. Improving the spectral unmixing algorithm to map water turbidity Distributions. *Environ. Model. Softw.* **2009**, *24*, 1051–1061. [[CrossRef](#)]
49. USGS. LPDAAC Data Pool. Available online: https://lpdaac.usgs.gov/data_access/data_pool (accessed on 27 April 2016).
50. Dell Software. Available online: <https://www.statsoft.com> (accessed on 27 April 2016).
51. Wang, M.; Tang, J.; Shi, W. MODIS-derived ocean color products along the China east coastal region. *Geophys. Res. Lett.* **2007**, *34*, L06611. [[CrossRef](#)]
52. Cui, L.; Zhai, Y.; Wu, G. Dredging being moved southward enlarges the impacted region in Poyang Lake—The evidences from multi-remote sensing images. *Acta Ecol. Sin.* **2013**, *11*, 3520–3525. (In Chinese)
53. Wu, G.; Cui, L.; Duan, H.; Fei, T.; Liu, Y. Specific absorption and backscattering coefficients of the main water constituents in Poyang Lake, China. *Environ. Monit. Assess.* **2013**, *185*, 4191–4206. [[CrossRef](#)] [[PubMed](#)]
54. Doxaran, D.; Cherukuru, N.; Lavender, S.J. Apparent and inherent optical properties of turbid estuarine waters: measurements, empirical quantification relationships, and modeling. *Appl. Opt.* **2006**, *45*, 2310–2324. [[CrossRef](#)] [[PubMed](#)]
55. Lee, Z.P.; Carder, K.L.; Arnone, R.A. Deriving inherent optical properties from water color: A multiband quasi-analytical algorithm for optically deep waters. *Appl. Opt.* **2002**, *41*, 5755–5772. [[CrossRef](#)] [[PubMed](#)]
56. Ma, R.; Tang, J.; Dai, J. Bio-optical model with optimal parameter suitable for Taihu Lake in water colour remote sensing. *Int. J. Remote Sens.* **2006**, *27*, 4305–4328. [[CrossRef](#)]
57. Shi, W.; Wang, M. An assessment of the black ocean pixel assumption for MODIS SWIR bands. *Remote Sens. Environ.* **2009**, *113*, 1587–1597. [[CrossRef](#)]
58. Wang, M.H.; Shi, W. The NIR-SWIR combined atmospheric correction approach for MODIS ocean color data processing. *Opt. Express* **2007**, *15*, 15722–15733. [[CrossRef](#)] [[PubMed](#)]
59. Wang, M.H.; Son, S.; Shi, W. Evaluation of MODIS SWIR and NIR-SWIR atmospheric correction algorithms using SeaBASS data. *Remote Sens. Environ.* **2009**, *113*, 635–644. [[CrossRef](#)]
60. Wang, M.H.; Shi, W.; Jiang, L.D. Atmospheric correction using near-infrared bands for satellite ocean color data processing in the turbid western Pacific region. *Opt. Express* **2012**, *20*, 741–753. [[CrossRef](#)] [[PubMed](#)]
61. Zheng, Z.B.; Li, Y.M.; Guo, Y.L.; Xu, Y.F.; Liu, G.; Du, C.G. Landsat-Based Long-Term Monitoring of Total Suspended Matter Concentration Pattern Change in the Wet Season for Dongting Lake, China. *Remote Sens.* **2015**, *7*, 13975–13999. [[CrossRef](#)]

